2009

Landscape Structure Control on Soil CO_2 Efflux Variability in Complex Terrain: Scaling from Point Observations to Watershed Scale Fluxes

Diego Andrés Riveros-Iregui
University of Nebraska - Lincoln, driveros2@unl.edu

Brian L. McGlynn
University of Colorado, Boulder

JOURNAL OF GEOPHYSICAL RESEARCH, VOL. 114, G02010, doi:10.1029/2008JG000885, 2009

Landscape structure control on soil CO_2 efflux variability in complex terrain: Scaling from point observations to watershed scale fluxes

Diego A. Riveros-Iregui[1,2] and Brian L. McGlynn[1]

Received 3 November 2008; revised 4 March 2009; accepted 13 March 2009; published 15 May 2009.

[1] We investigated the spatial and temporal variability of soil CO_2 efflux across 62 sites of a 393-ha complex watershed of the northern Rocky Mountains. Growing season (83 day) cumulative soil CO_2 efflux varied from ~300 to ~2000 g CO_2 m^{-2}, depending upon landscape position, with a median of 879.8 g CO_2 m^{-2}. Our findings revealed that highest soil CO_2 efflux rates were observed in areas with persistently high soil moisture (riparian meadows), whereas lower soil CO_2 efflux rates were observed on forested uplands (98% of watershed area). Furthermore, upslope accumulated area (UAA), a surrogate measure of the lateral redistribution of soil water, was positively correlated with seasonal soil CO_2 efflux at all upland sites, increasing in explanatory power when sites were separated by the major aspects of the watershed (SE/NW). We used the UAA–soil CO_2 efflux relationship to upscale measured CO_2 efflux to the entire watershed and found watershed-scale soil CO_2 efflux of 799.45 ± 151.1 g CO_2 m^{-2} over 83 days. These estimates compared well with independent eddy covariance estimates of nighttime ecosystem respiration measured over the forest. We applied this empirical model to three synthetic watersheds with progressively reduced complexity and found that seasonal estimates of soil CO_2 efflux increased by 50, 58, and 98%, demonstrating the importance of landscape structure in controlling CO_2 efflux magnitude. Our study represents an empirical quantification of seasonal watershed-scale soil CO_2 efflux and demonstrates that UAA (i.e., landscape position) and drainage patterns are important controls on the spatial organization of large-scale (~km^2) soil CO_2 efflux, particularly in semiarid, subalpine ecosystems.

Citation: Riveros-Iregui, D. A., and B. L. McGlynn (2009), Landscape structure control on soil CO_2 efflux variability in complex terrain: Scaling from point observations to watershed scale fluxes, *J. Geophys. Res.*, *114*, G02010, doi:10.1029/2008JG000885.

1. Introduction

[2] Soil CO_2 efflux, also known as soil respiration, is an important component of the C cycle, and its accurate quantification has significant implications for ecosystem C balances and models [*Raich and Schlesinger*, 1992; *Raich and Potter*, 1995; *Valentini et al.*, 2000]. One obstacle to accurately quantifying soil CO_2 efflux is the large spatial heterogeneity in the physical and biogeochemical processes leading to soil CO_2 production and efflux. Particularly in complex terrain, interactions among spatially variable soil temperature, soil water content, vegetation, substrate, and soil physical properties induce large heterogeneity in the magnitude of soil CO_2 efflux [*Kang et al.*, 2003, 2006; *Scott-Denton et al.*, 2003]. Further complications are introduced by the superimposed temporal heterogeneity (asynchronous responses of soil CO_2 to each controlling variable). As a result, estimating soil CO_2 efflux from large areas has proven problematic [*Goulden et al.*, 1996], commonly leading to highly uncertain estimates.

[3] Many of the known estimates of soil CO_2 efflux rates from entire watersheds come from area-weighed extrapolations of measurements at single or few sites [e.g., *Norman et al.*, 1992; *Lavigne et al.*, 1997; *Ryan et al.*, 1997; *Webster et al.*, 2008a]. However, little assessment has tested the representativeness of such sites for the entire area of study. Other studies use temperature-based relationships to model soil CO_2 efflux rates for large areas [*Hollinger et al.*, 1994; *Randerson et al.*, 2002; *Richardson et al.*, 2006; *Larsen et al.*, 2007], providing useful estimates for comparison with other techniques (e.g., eddy covariance). However, through this or similar exercises little understanding can be gained about the variability of processes occurring within these areas. Despite the number of studies measuring rates of soil CO_2 efflux, studies addressing the heterogeneity of this flux at large scales (e.g., watershed scale (~km^2)) using ground-based measurements, or studies taking into account the effects of landscape heterogeneity remain limited.

[4] Watershed morphology and heterogeneity can exert important influences on the magnitude of soil CO_2 efflux rates. For example, physical organization of landscapes is manifested in aspect variations and differences in surface

[1]Department of Land Resources and Environmental Sciences, Montana State University, Bozeman, Montana, USA.
[2]Department of Ecology and Evolutionary Biology, University of Colorado, Boulder, Colorado, USA.

0148-0227/09/2008JG000885$09.00

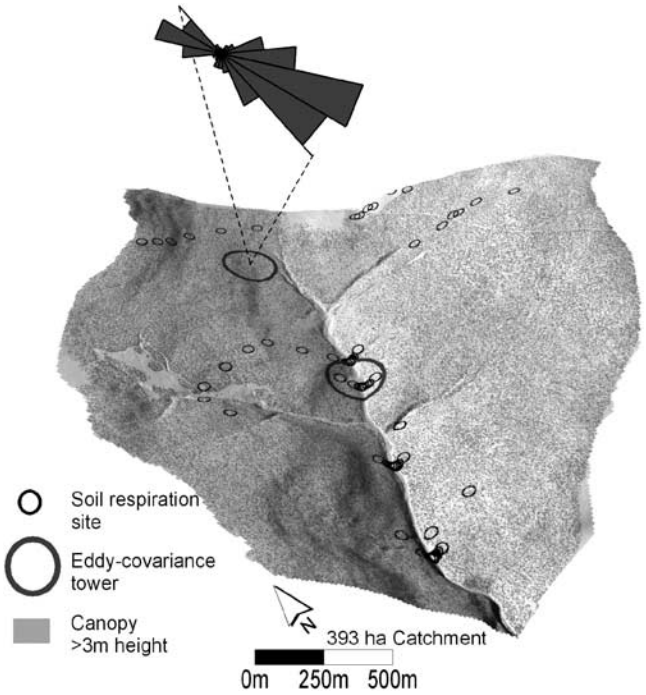

Figure 1. Distribution of 62 sites across Stringer Creek watershed. Stringer Creek is located in the Tenderfoot Creek Experimental Forest, in the Little Belt Mountains of central Montana. Stringer Creek watershed is ~393 ha in area. Wind rose indicates predominant wind direction for the period between 9 June and 30 August 2006.

energy balance distributions across a watershed. Radiation differences have been found to influence spatial variation of temperature [*Korkalainen and Lauren*, 2006], and vegetation and litter accumulation [*Stage*, 1976; *Webster et al.*, 2008a], which in turn can result in differences in soil carbon content. Concurrently, landscape structure (shape) and gravity exert a major control in the vertical and lateral redistribution of water in the soil, which typically defines wet and dry areas of the landscape [*Western et al.*, 1998, 1999]. In fact, wetness differences have been found to control differences in soil CO_2 fluxes [*Riveros-Iregui et al.*, 2008] partially because plant and microbial activities are dependent on soil water content, and transport (diffusivity) of soil CO_2 is inversely correlated with soil water content [*Riveros-Iregui et al.*, 2007; *Pacific et al.*, 2008].

[5] Given the spatiotemporal heterogeneity of soil CO_2 efflux, estimating soil CO_2 efflux rates from entire watersheds requires thorough understanding of the biophysical and landscape controls. Spatially, soil CO_2 efflux can vary across topographic positions [*Pacific et al.*, 2008; *Riveros-Iregui et al.*, 2008; *Webster et al.*, 2008b], aspect [*Webster et al.*, 2008a], vegetation cover [*Scott-Denton et al.*, 2003, 2006; *Tang et al.*, 2005], and across different land uses [*Jacobs et al.*, 2007; *Nouvellon et al.*, 2008]. Temporally, soil CO_2 efflux can vary with changing hydrologic [*Riveros-Iregui et al.*, 2007; *Pacific et al.*, 2008] and climatic conditions [*Vargas and Allen*, 2008]. Given the broad range of landscape elements that can exist within a single watersheds (e.g., riparian meadows, forested hillslopes, contrasting aspects), and owing to the different responses that soil CO_2 efflux can exhibit to different environmental conditions (e.g., precipitation, seasonal drying of the soil, temperature), it is important to determine the overarching control on soil CO_2 efflux across large and heterogeneous areas. Investigating and quantifying the fundamental role of landscape-induced heterogeneity on soil CO_2 production and efflux can improve our understanding of the variability of this flux at the watershed scale, and reduce the uncertainty in estimates of soil CO_2 efflux from heterogeneous areas.

[6] We investigated the spatial and temporal variability of soil CO_2 efflux across 62 sites in the northern Rocky Mountains. The sites were distributed across a 393-ha, moderately complex watershed and were characteristic of the spatial heterogeneity of the landscape (e.g., slope, aspect, upslope accumulated areas). This forest is ideal for coupled hydrologic–soil CO_2 efflux research as it exhibits the full range in soil water content, soil temperature, soil nutrient status, and vegetation cover, and is characteristic of subalpine watersheds in the northern Rocky Mountains. The objectives of this study were to (1) evaluate growing season (June thru August, 2006) soil CO_2 efflux across 62 landscape positions and quantify its spatial heterogeneity; (2) assess the role of landscape structure and drainage patterns on controlling the magnitude of soil CO_2 efflux; and (3) present an empirical framework for quantifying large-scale (km^2) soil CO_2 efflux rates for complex terrain watersheds. The information presented here is essential to linking plot-scale observations to large-scale estimates of soil CO_2 efflux, to enhancing parameterization and modeling of soil CO_2 efflux from heterogeneous areas, and is useful in combination with other ecosystem-level measures of C exchange (e.g., flux towers).

2. Methods

2.1. Study Site

[7] This study was located in the Tenderfoot Creek Experimental Forest (TCEF), in the Little Belt Mountains of central Montana (46°55 N; 110°54 W). This location is characteristic of the lodgepole-dominated forests of the northern Rocky Mountains, believed to contribute significantly to the North American carbon sink [*Schimel et al.*, 2002]. The greater TCEF elevation ranges from 1840 to 2421 m and has an area of 3591 ha. Mean annual precipitation is 880 mm with 70% falling as snow [*Farnes et al.*, 1995], and peak snowpack accumulations occur between late March and mid-April [*Woods et al.*, 2006]. Mean annual temperature is 0°C, and the growing season typically extends from early or mid-June to the end of August. A 393-ha subwatershed that contains a second-order perennial stream, Stringer Creek, was selected as the watershed of interest owing to its wide range of slope, aspect, and topographic convergence/divergence. Within the Stringer Creek watershed, we selected 62 sites to measure soil CO_2 efflux via a combination of 5 upland and 4 upland-riparian-upland (URU) transects distributed across the watershed (Figure 1). Each upland transect contained between 4 and 6 sites, whereas each URU transect contained 8 sites, for a combined total of 62 sites (11 riparian meadow sites, 51 upland forest sites) across Stringer Creek watershed. Because our goal was to examine the variability of soil CO_2 efflux in response to differences in biophysical controls

Table 1. C:N Content Ratio of Riparian and Upland Vegetation at Stringer Creek[a]

Riparian Meadows			Upland Forests		
Type	C:N Ratio	SD	Type	C:N Ratio	SD
Calamagrostis – shoots	17.9	1.0	*Vaccinium* – leaves	19.5	0.7
Calamagrostis – roots	31.6	11.5	*Vaccinium* – stems	57.6	2.1
Urtica dioica – shoots	11.4	1.0	*Vaccinium* – roots	87.0	11.2
Urtica dioica – roots	20.5	1.3	*Deschampsia cespitosa* – shoots	44.3	0.8
			Deschampsia cespitosa – roots	70.8	12.7
			Pinus contorta – twigs	129.7	7.7
			Pinus contorta – roots	172.2	12.9
			Pinus contorta – live needles	54.0	8.2
			Pinus contorta – dead needles	58.5	8.6

[a]Values represent the means of three samples and one standard deviation of the means. Vegetation description is after *Mincemoyer and Birdsall* [2006].

(e.g., soil temperature, soil water content, vegetation cover), site selection was targeted toward those areas of the landscape that offered natural biophysical gradients, while maintaining the practicality of daily to subweekly manual measurements at each site. Terrain analysis confirmed that site selection was characteristic of the distribution of upslope accumulated area (an indicator of landscape variability) across the watershed (see section 3). Additional details on site characteristics have been described in previous studies [*Riveros-Iregui et al.*, 2007, 2008; *Riveros-Iregui*, 2008].

2.2. Terrain Variability

[8] A 1-m digital elevation model (DEM) derived from Airborne Laser Swath Mapping (courtesy of the National Center for Airbone Laser Mapping (NCALM)) was resampled to 3-m and 10-m DEMs for Stringer Creek. The resampled DEMs were then used to calculate upslope accumulated area (UAA (m^2)) for each pixel in the watershed, on the basis of the triangular multiple flow direction algorithm (MD∞) [*Seibert and McGlynn*, 2007]. Also known as the local contributing area, UAA represents the amount of area draining to a specific location in the landscape [*Beven et al.*, 1979; *McGlynn and Seibert*, 2003] and serves as an estimate of relative wetness potential. This and similar topographic indices have proven useful for comparison of soil moisture patterns among sites of the same watershed [*Burt and Butcher*, 1985; *Western and Grayson*, 1998; *Western et al.*, 1999; *Grayson and Western*, 2001] and across larger regions [*Rodhe and Seibert*, 1999; *Zinko et al.*, 2005; *Sorensen et al.*, 2006]. Riparian zone delineation was accomplished using a 3-m elevation threshold above the stream channel following flow paths to the stream, according to the delineation algorithm proposed by *McGlynn and Seibert* [2003], and corroborated with field observations and measurements [*Jencso et al.*, 2009].

2.3. Environmental Variables

[9] We report on a set of measurements of soil temperature (T_S) and volumetric soil water content (θ) recorded during the 2006 growing season. Continuous measurements of T_S were recorded every 4 h at 13 of the 62 sites at 5 cm depth with iButton temperature loggers (DS1922L, temperature range −40°C to 85°C, measured accuracy better than 0.5°C between −20 and 40°C, Maxim Integrated Products, Sunnyvale, California), during the period between 17 July and 16 October 2006. Once deployed, iButtons were not retrieved until the end of the experiment to avoid soil disturbance. On the basis of these measurements, we calculated the number of days that average daily T_S rose above the mean T_S at all 13 sites. Although analyzed at only 13 sites, this estimate allowed for comparison between SE and NW facing areas of the landscape, providing an assessment of variability of T_S at the watershed scale throughout the growing season.

[10] Continuous measurements of θ were made using water content reflectometry probes (CSI Model 616, Campbell Scientific Inc., Logan, Utah) at three sites (riparian meadow, lower hillslope, and upper hillslope) installed horizontally at 20 cm. Given the large data set of T_S and θ measurements, our results are summarized to illustrate distinct dynamics of these variables at the watershed scale.

2.4. Soil C:N Content Ratio, Biomass C:N Content Ratio, and Fine Root Biomass

[11] Soil carbon and nitrogen content ratios (C:N) were measured in a subset of sites (45), including riparian meadow sites and upland forest sites. Soil samples were collected by sampling the top 25 cm of soil with a hand auger (5 cm in diameter). In the lab, samples were dried, sieved, and ground in preparation for analysis. Total C and N contents were determined in a TruSpec CN Determinator (Leco Corporation, St. Joseph, Michigan) through combustion under an oxygen atmosphere at 950°C, using helium as a carrier. This instrument has a precision of 0.3 ppm for C and 40 ppm for N. Additionally, aboveground and belowground biomass of the dominant vegetation from riparian meadows and upland forests was collected for similar C:N content ratio analysis (Table 1). Results are presented as the mean and one standard deviation of three measurements.

[12] Fine root biomass ($\leq$0.5 cm in diameter) was quantified at 19 of the 62 sites by sampling the top 25 cm of soil with a hand auger (5 cm in diameter). Soil cores were collected in triplicate and dried at 60°C, and roots were manually separated and weighed. Estimates of fine root density are presented as the mean and one standard deviation of three measurements [kg m^{-3}].

2.5. Soil CO_2 Efflux

[13] Each of the 62 sites consisted of a 0.5-m^2 area flux plot, roped off to minimize disturbance. Soil CO_2 efflux measurements were collected using a soil respiration chamber model SRC-1 (footprint of 314.2 cm^2, accuracy within 1% of calibrated range [0 to 9.99 g CO_2 m^{-2} hr^{-1}], PP Systems, Massachusetts) equipped with an infrared gas analyzer (IRGA; EGM-4, accuracy within 1% of calibrated

range [0 to 2,000 ppm], PP Systems, Massachusetts). Chamber measurements were collected at each of the 62 sites following similar procedures to those described by *Pacific et al.* [2008] and *Riveros-Iregui et al.* [2008]. Before each measurement the soil chamber was flushed with ambient air for 15 s, placed onto the soil plot, and gently inserted ~1 cm in the soil to ensure a good seal between the chamber and the soil surface. Following manufacturer's recommendations, soil CO_2 efflux was calculated by measuring the rate of increase in CO_2 concentration within the chamber and fitting a quadratic equation to the relationship between the increasing CO_2 concentration and elapsed time. The deployment of the chamber lasted for 120 s or until the internal chamber CO_2 concentration increased by 60 ppm, time after which a direct reading of the flux rate was taken from the IRGA. Chamber measurements were collected in triplicate at each plot between 1000 h and 1600 h every 2–7 days. Above ground vegetation was clipped once a week after measurements were taken, and roots were left intact to avoid disturbance.

[14] Owing to the broad spatial distribution of the sites and travel time across the 393-ha study site, soil CO_2 efflux was not measured at every site on the same day or at the same time of the day. Thus, throughout the 2006 growing season, each site was visited between 10 and 37 times. Here we focus on seasonal estimates (cumulative fluxes) across all sites, as important indicators of the heterogeneity (and magnitude) of soil CO_2 efflux across the watershed. We established a common timeframe among sites by linearly interpolating between measurements for the time period 9 June 2006 and 30 August 2006 (83 days total). In a previous study, we compared high- and low-frequency measurements and demonstrated that sampling frequency, linear interpolation between measurements, and time of day do not compromise or bias estimates of soil CO_2 efflux when analyzed cumulatively (seasonally) [*Riveros-Iregui et al.*, 2008]. Our approach provided a robust framework for intersite comparison of seasonal fluxes, while optimizing resources, manual labor, and measurements across 62 spatially distributed sites.

[15] Analysis of variance revealed that cumulative soil CO_2 effluxes in riparian sites were significantly higher than in upland sites ($p \ll 0.001$). Yet to further analyze the dynamics of efflux over the course of the entire growing season, we applied a two-way partitioning algorithm (k-means Clustering, Matlab 7.4.0, The Mathworks, Inc.) to the entire soil CO_2 efflux data set. A two-way partition was chosen as a first approach to separate the 62 sites into two groups (a cluster of sites with high soil CO_2 efflux, and a cluster of sites with low soil CO_2 efflux) and to answer a fundamental question: are observed soil CO_2 effluxes in agreement with terrain analysis and delineation between riparian and upland sites? The selected algorithm separates all observations into two mutually exclusive clusters, using an iterative minimization of the sum of the distances from each data point to its cluster centroid, and relocating data points between clusters until the sum cannot be decreased any further [*Spath*, 1985]. The use of the two-way partitioning algorithm in this manner also allowed for independent categorization of riparian and upland sites (previously mapped through terrain analysis). The algorithm is suitable for clustering time series of CO_2 efflux from multiple sites, because it takes into account the distribution and behavior (dynamics) of the entire time series at each site.

2.6. Ecosystem Respiration

[16] Continuous measurements of land-atmosphere CO_2 and water vapor exchange were made above the canopy of both riparian grasses and upland forests (Figure 1) with the eddy covariance method [*Baldocchi*, 2003]. Wind velocity was measured with a triaxial sonic anemometer (CSAT3, Campbell Scientific Inc., Logan, Utah), whereas CO_2 and water vapor were measured with an open path, infrared absorption gas analyzer (7500, LI-COR, Lincoln, Nebraska) at 10 Hz frequencies. Estimates of nighttime ecosystem respiration were selected on the basis of fluxes between 2300 and 0400 LT and reported on a 24-h basis, using a U^* threshold of 0.2 m s^{-1} to ensure periods with enough turbulence. Because the purpose of the eddy covariance measurements was exclusively to provide a relative comparison, values are presented as nighttime ecosystem respiration fluxes, and no daytime correction was applied to fluxes.

3. Results

3.1. Terrain Variability

[17] Riparian delineation of the Stringer Creek watershed demonstrated that riparian zones comprised 1.8% of the watershed. The rest of the watershed was divided almost symmetrically by the stream, which runs in a NNE–SSW direction, making NW and SE the two dominant aspects of the watershed (50.0 and 48.2%, respectively). The 3-m DEM provided a more accurate representation of the microscale (e.g., fallen trees, stream channel, man-made structures) at each particular plot (soil CO_2 efflux plots were 0.5 m^2 in area), whereas the 10-m DEM of Stringer Creek provided the most robust representation of landscape structure and morphology (convergent versus divergent areas) without being biased by the microtopography. Thus, we used the 3-m DEM for assessment of UAA for all measurement locations, regressions and upscaling, whereas the calculated 10-m upslope accumulated area (UAA) served as a general landscape position characterization of sites across the watershed (Figure 2).

[18] On the basis of these topographic variables (UAA, aspect), found to control the redistribution of water and radiation received across the watershed, we evaluated the representativeness of the selected 62 sites to the entire watershed. Terrain analysis confirmed that the selected 62 sites were characteristic of both UAA distribution and aspect (Figure 2), demonstrating that site selection captured the range and frequency of landscape positions, drainage patterns, and overall complexity of the Stringer Creek watershed.

3.2. Environmental Variables

[19] The average soil temperature (T_S) of all measured sites was 8.97°C between 17 July and 16 October 2006; however T_S varied widely across the watershed from near ~30°C during the summer in well-exposed areas (riparian meadows) to below freezing in October. Average T_S in riparian meadow sites was 10.21°C, with 21.5 days above the mean T_S for the watershed (Figure 3). SE facing forested

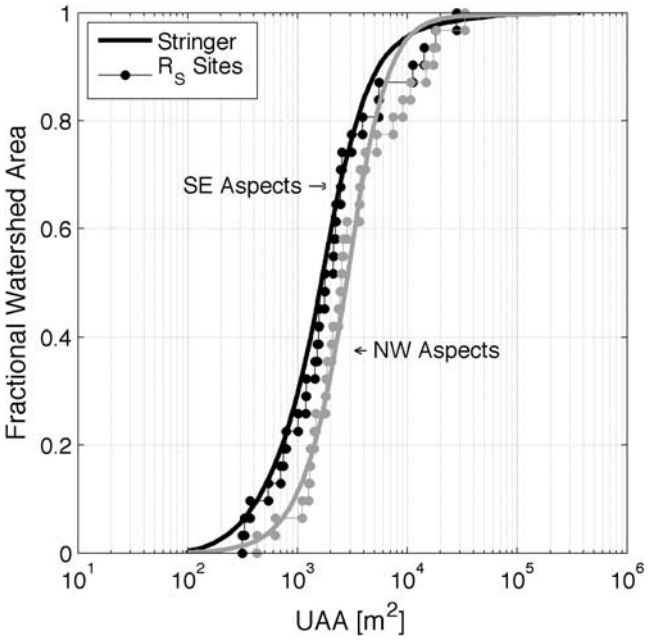

Figure 2. Distribution of 10-m upslope accumulated area (UAA) across Stringer Creek watershed (continuous lines) and across sites where soil CO_2 efflux (R_S) was measured. Sites were separated by aspect into the two main categories: SE (black) and NW (gray) facing aspects. This analysis demonstrates that the selected sites were characteristic of the distribution of UAA for the Stringer Creek watershed.

upland sites showed an average T_S of 8.83°C, with 14.4 days above the mean for the watershed. NW facing forested upland sites showed an average T_S of 7.89°C, with only 2.5 days above the mean for the watershed (Figure 3). In general, three major features were observed to control T_S at the watershed scale: (1) a vegetation effect, in which T_S was buffered in areas with tall canopies (e.g., riparian meadow versus forested uplands); (2) an aspect effect, in which SE facing sites received more solar radiation than NW facing sites causing differences in amplitude of T_S between aspects; and (3) a soil water content effect (specific heat effect), in which T_S had less diel amplitude in wetter areas of the landscape (lower areas) than in upper areas (drier areas). While other physical effects may also control T_S at smaller scales, these effects illustrate the main observed controls on watershed-scale variability of T_S.

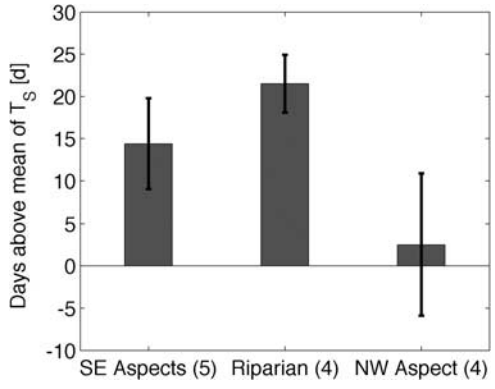

Figure 3. Degree days above the mean for sites in SE aspects (5), riparian meadows (4), and NW aspects (4), based on 4-h measurements from 17 July to 16 October 2006. Mean is from data at all sites. Bar heights indicate the mean of degree days at sites within each landscape element and error bars one standard deviation of degree days of each site.

[20] Highest values of volumetric soil water content (θ) were observed toward mid-May and early June following snowmelt, after which values of θ decreased at all sites (Figure 4). Snowmelt lasted until mid-May, whereas liquid precipitation was high during June and early July and decreased toward late July and August (Figure 4). Spatially, values of θ reached ~0.5 m^3 m^{-3} (i.e., at or near soil saturation) in low and convergent areas of the landscape (riparian zones) immediately after snowmelt. Values of θ were lower in less convergent areas and higher landscape positions (reduced drainage area), where maximum values did not exceed ~0.2 m^3 m^{-3} (Figure 4).

3.3. Soil C:N Content Ratio, Biomass C:N Content Ratio, and Fine Root Biomass

[21] Soil C:N content ratios varied from ~10 to ~40 among the 45 sampled sites of the watershed (Figure 5a). Spatially, soil C:N content ratio was negatively correlated to the ratio of UAA and the tangent of local slope, β ($r^2 = 0.38$; $p < 0.001$), meaning that areas of the landscape that are relatively wetter had a lower soil C:N content ratio than those areas of the landscape that are relatively drier. Also known as the topographic index [*Beven and Kirkby*, 1979], the slope-normalized UAA represents a widely applied estimate for relative wetness. While similar trends can be observed when using C and N alone, combined C:N ratios displayed the strongest relationship with topographic index. Biomass C:N content ratio varied among species and among aboveground and belowground biomass of riparian mead-

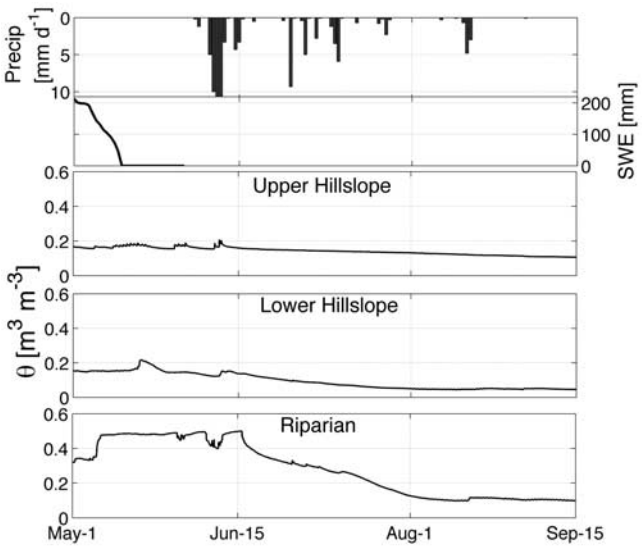

Figure 4. Variability of precipitation, snow water equivalent (SWE), and soil water content (θ) at 20 cm across high and low hillslopes and a riparian meadow of Stringer Creek watershed for the 2006 growing season.

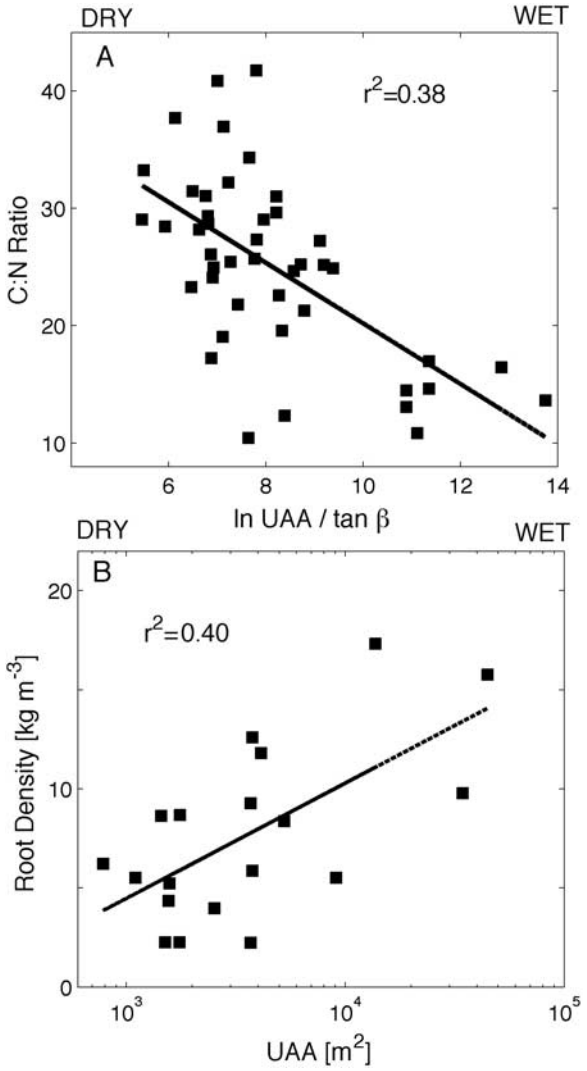

Figure 5. (a) Relationship between topographic index (the ratio of UAA and the tangent of local slope (β)) and C and N content in the soil. (b) Relationship between root density (kg m^{-3}) and UAA. Note the log scale for the *x* axis.

ows and upland forests as shown in Table 1. In general, lodgepole pine (*Pinus contorta*) from upland forests had a C:N content ratio between 5 and 10 times higher than C:N content ratio of riparian meadow grasses.

[22] Fine root biomass varied from ~2 to ~18 kg m^{-3} across the 19 sampled sites of the watershed (Figure 5b). Spatially, fine root biomass was positively correlated with UAA ($r^2 = 0.40$; $p < 0.001$), meaning that wetter areas of the landscape had a higher content of fine roots than dry areas. These relationships (as presented in Figure 5) suggest that these biophysical variables, known to influence soil CO_2 production and efflux, are also topographically organized and their spatial variability is partially mediated by landscape structure.

3.4. Soil CO_2 Efflux

[23] Seasonal estimates (83-day accumulations) of soil CO_2 efflux during the 2006 growing season were highly variable across the 62 sampled sites of the watershed (Figure 6a). Soil CO_2 efflux varied from ~300 g CO_2 m^{-2} to ~2000 g CO_2 m^{-2}, depending upon landscape position. At first glance, there is a sevenfold difference in effluxes across this montane watershed, with a median of 879.8 g CO_2 m^{-2}. To examine soil CO_2 efflux behavior over the course of the entire growing season, we applied a two-way partitioning algorithm (k-means, see section 2) to the time series of all 62 sites. This algorithm separated the 62 sites into two clusters (Figure 6b) with centroids of 839 and 1555 g CO_2 m^{-2}, respectively. Our results revealed that 14 sites were clustered with the higher centroid value, whereas 48 sites were clustered with the lower centroid value (Figure 6b). Analysis of the landscape position of each site demonstrated that 11 out of the 14 sites of the higher cluster corresponded to riparian meadow sites, and conversely, sites located in the uplands were consistently classified within the lower centroid values (Figure 6b). Two of the remaining three sites of the high cluster were located on low hillslopes adjacent to riparian meadows (areas prone to high soil water content), and the third one was located in an elevated NW facing site. Given the consistent high effluxes from this elevate NW facing site, we believe that this anomalous site was located immediately above a large root or series of roots and received respiration very rapidly from the source.

[24] In summary, k-means clustering revealed that the highest soil CO_2 efflux rates were observed in areas with persistent high soil water content (riparian meadows), whereas lower soil CO_2 efflux rates were observed on upland forests (Figure 6b). Given the consistent differences in CO_2 efflux between riparian meadows and upland forests based on landscape position ($p \ll 0.001$) and the overwhelming fraction of uplands relative to total area (~98%), we investigated the effects of landscape position on soil CO_2 efflux within upland sites. Using the UAA layer calculated from the 3-m DEM, as a measure of the lateral redistribution of soil water caused by local topography, we found a positive correlation between UAA and cumulative soil CO_2 efflux at all sites ($r^2 = 0.51$; $p < 0.001$; Figure 7). However, the explanatory power of UAA considerably increased when sites were separated by the two major aspects of this watershed: SE aspects ($r^2 = 0.65$; $p < 0.001$) and NW aspects ($r^2 = 0.61$; $p < 0.001$; Figure 7), suggesting that the lateral redistribution of soil water and soil temperature as mediated by landscape structure can control soil CO_2 efflux in upland sites.

[25] We used these relationships (Figures 6 and 7) to upscale measured soil CO_2 efflux to the entire watershed via a two-step approach. First, we discretized the landscape into riparian meadows and upland forests. We area weighed mean efflux from riparian meadows (1572.1 g CO_2 m^2 over 83 days from 1.8% of the watershed). Second, we applied the UAA–soil CO_2 efflux relationships found for upland sites (Figure 7) to the entire distribution of UAA for this watershed. We found that soil CO_2 efflux from SE aspects (48.2% of the watershed) was of 730.5 ± 207.1 g CO_2 m^2 over 83 days, whereas soil CO_2 efflux in NW aspects (50.0% of the watershed) was 838.4 ± 102.5 g CO_2 m^2 over 83 days. In combination with efflux from riparian meadows, our study found watershed-scale soil CO_2 efflux of 799.45 ± 151.1 g CO_2 m^2 over 83 days (Table 2). These estimates represent an important step to quantifying water-

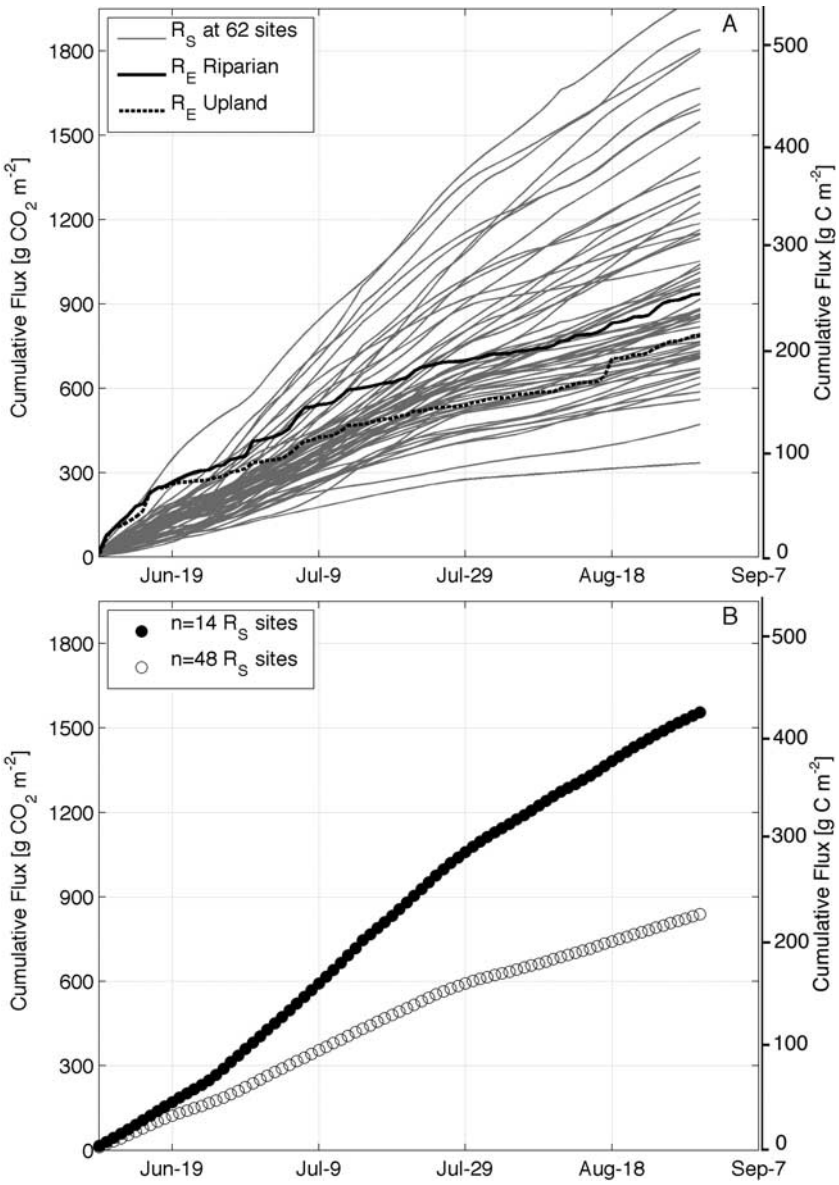

Figure 6. (a) Variability of cumulative 83-day soil CO_2 efflux (R_S) across 62 sites in Stringer Creek watershed during the 2006 growing season. Note an approximately sevenfold difference in estimates of soil CO_2 efflux across the watershed. Nighttime ecosystem respiration fluxes (R_E) from the riparian and the upland towers are shown for context. (b) Partitioning of sites using cluster analysis demonstrates that 14 sites are classified within the cluster with the higher centroid value (filled circles); 11 of these sites are located in the riparian meadow. Sites located in the hillslopes are consistently classified within the lower centroid values (open circles).

shed-scale soil CO_2 efflux, on the basis of empirical relationships developed from repeated measurements of soil CO_2 efflux and landscape structure characteristics.

4. Discussion

[26] In past investigations, when more than a few data collection sites were located in a given area, they were limited in number and distribution with little assessment of how well characterized the sampling sites were to the rest of the study area. With a wealth of literature on soil CO_2 efflux, studies addressing watershed-scale soil CO_2 efflux remain limited. Furthermore, poor temporal resolution of measurements at a small number of sites has further restricted understanding of how soil CO_2 production and efflux change over space and time. Thus, serious complications can arise when, on the basis of limited measurements at potentially biased spatial locations, attempts are made to spatially upscale soil CO_2 efflux. The result is often a modeling approach (e.g., soil CO_2 efflux as a function of soil temperature or solar radiation) [*Fox et al.*, 2008] that allows for temporal extrapolation, and another modeling approach applied on the spatial scale (e.g., as a function of landscape cover or vegetation index [*Vourlitis et al.*, 2000; *Kim et al.*, 2006] or an area-weighted sum of fluxes at single

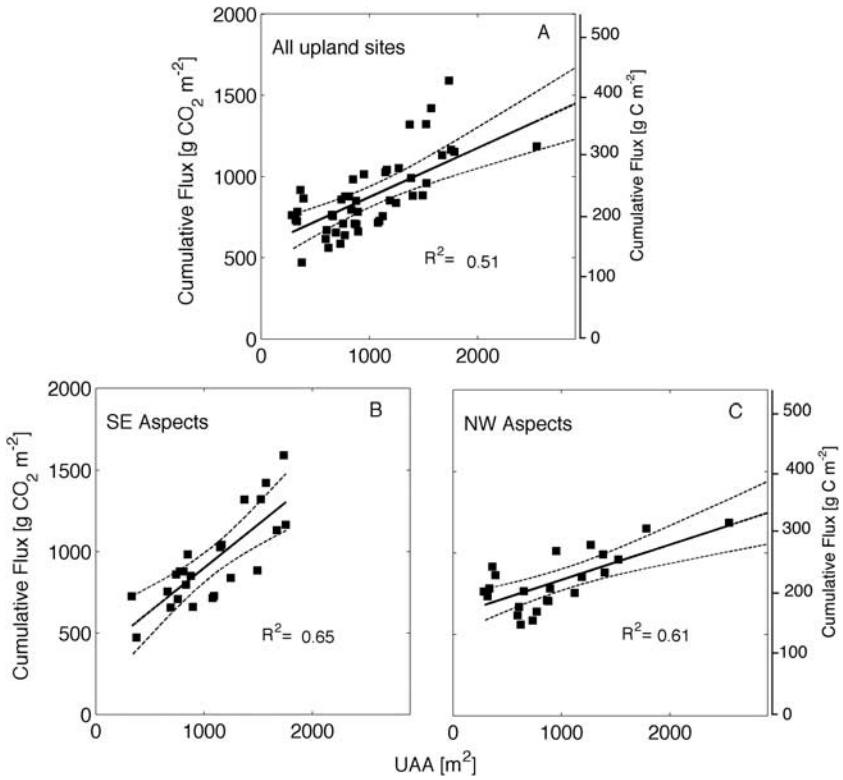

Figure 7. Relationship between calculated 3-m UAA and cumulative soil CO_2 flux (R_S) at (a) all upland sites and (b and c) separated by aspect. The relationship for SE aspects was $R_S = (0.534 \times UAA) + 366.9$. The relationship for NW aspects was $R_S = (0.217 \times UAA) + 619.4$. Dashed lines represent the Working-Hotelling 95% confidence band of each regression line.

or few locations [*Soegaard et al.*, 2000; *Heikkinen et al.*, 2004; *Webster et al.*, 2008a]). Given the uncertainty in each of these modeling exercises due to limited and/or biased data, watershed-scale estimates of soil CO_2 efflux have not yet been rigorously accomplished.

[27] In this study, we have demonstrated that the selected 62 measurement sites well characterized the topographic heterogeneity of Stringer Creek watershed (Figure 2), therefore we suggest that spatially, there was little bias introduced during site selection and sampling design. Temporally, our repeated measurements varied from 10 to 37 chamber measurements across 62 sites. Previously demonstrated for this subalpine ecosystem [*Riveros-Iregui et al.*, 2008], measurements taken between 1000 and 1600 h introduced little time of day bias and frequency bias when estimates are analyzed seasonally (cumulatively), primarily because the seasonality soil CO_2 efflux induced by changes of soil water prevails over diel dynamics driven by soil temperature and plant activity [*Riveros-Iregui et al.*, 2007, 2008]. Thus, our soil CO_2 efflux measurements characterized both the spatial heterogeneity and temporal variability of effluxes throughout the 83-day period across this northern Rocky Mountain watershed.

4.1. Environmental Variables and Landscape Structure

[28] One of the outstanding issues in C cycle research and specifically for soil CO_2 efflux is understanding the spatial and temporal heterogeneity induced by landscape structure. Landscape morphology imposes organized heterogeneity on soil temperature and on the allocation/redistribution of water and ultimately soil water content, and this is reflected not only on soil CO_2 efflux but also on its other biophysical controls (e.g., aboveground and belowground biomass, C:N content ratios). While the timing of snowmelt can differ from year to year depending on the snow energy balance and snowpack accumulation, the spatial pattern of soil water content (θ) is imposed by landscape morphology and structure. Thus, convergent areas (e.g., riparian meadows, convergent slopes) are likely to represent the higher values of θ within a watershed, whereas divergent areas (e.g., divergent slopes) tend to be drier. This results in a degree of predictability in patterns of soil water content on the basis of topographic position and landscape structure, and to a lower degree, patterns of soil temperature based on aspect, land cover, and surface energy balance. Understanding this structured heterogeneity is crucial for understanding soil organic matter accumulation, decomposition rates of C pools, and ultimately, rates of soil CO_2 production and efflux from heterogeneous areas. More broadly and importantly, the shape of the landscape and drainage patterns can impose structure on spatial heterogeneity of many biogeochemical processes mediated by soil temperature, soil water content, and the surface energy balance.

[29] In our study, measurements of soil C:N content ratio and fine root biomass were correlated to wetness indices (Figure 5) such as topographic index and upslope accumulated area [*Beven and Kirkby*, 1979; *Seibert and McGlynn*,

Table 2. Watershed-Scale Estimates of Seasonal Soil CO_2 Efflux for Stringer Creek Watershed and Three Synthetic Digital Elevation Models and Independent Estimates of Nighttime Ecosystem Respiration Measured Above the Canopy With an Eddy Covariance System

	Stringer Creek	Nighttime R_E	Watershed 1	Watershed 2	Watershed 3
Description	This study	*Riveros-Iregui et al.* [2008]	Convergent (bowl shaped)	Planar (steep slope)	Planar (gentle slope)
Calculated Riparian Area	1.8%	–	2.5%	0.34%	0.54%
Total soil CO_2 efflux (g CO_2 m^{-2} over 83 days)	799.5 ± 151.1	786.8	1199.8 ± 177.6	1261.9 ± 179.1	1584.1 ± 258.4

2007]. These wetness indices have been used in previous investigations as explanatory variables of hydrological and ecological correlations to topography [e.g., *Famiglietti and Wood*, 1991; *Rodhe and Seibert*, 1999; *Urban et al.*, 2000; *Guntner et al.*, 2004; *Lookingbill and Urban*, 2004; *Pierce et al.*, 2005; *Zinko et al.*, 2005; *Sorensen et al.*, 2006]. Wetter locations showed higher fine root biomass and lower C:N ratios, likely as the result of difference in vegetation cover (trees versus grasses, Table 1). Higher root biomass is known to contribute to higher soil CO_2 generation and flux [*Burton et al.*, 2000; *Maier and Kress*, 2000; *Pregitzer et al.*, 2000; *Shibistova et al.*, 2002], whereas lower C:N ratios are correlated to higher litter decomposition rates [*Bosatta and Staaf*, 1982; *Enriquez et al.*, 1993; *Fierer et al.*, 2006].

[30] Our findings also elucidate a much more intriguing and broader question: is there spatial and temporal organization in the contributions of autotrophic and heterotrophic respirations to total soil CO_2 efflux in subalpine ecosystems? Spatially, as evidenced from our results, fine root biomass and soil C:N ratios are organized topographically. Temporally, continuous measurements and the evolution of diel hysteresis patterns of soil CO_2 efflux across the season have been related to differences in the timing of autotrophic activity between one riparian and one upland site of this catchment [*Riveros-Iregui et al.*, 2008]. However, how this variability is spatially and temporally expressed across the 62 sites, or across the entire catchment, remains to be addressed. Nonetheless our findings set the stage (and highlight the need) for future research directed at separating autotrophic and heterotrophic respiration in a spatiotemporal manner.

4.2. How Does Soil CO_2 Efflux Vary Across Stringer Creek Watershed?

[31] While previous studies had demonstrated that soil CO_2 efflux can be highly variable across a few landscape positions [*Kang et al.*, 2003; *Saiz et al.*, 2006; *Webster et al.*, 2008b], little understanding has been provided about how topography and landscape structure can control soil CO_2 efflux and how this organized heterogeneity can be used for interpolation, extrapolation, and transfer. In our study, two-way k-means analysis revealed that a first-order categorization of the landscape can simply be made as a binary discretization: riparian meadows and forested uplands (Figure 6). Differences in efflux magnitude between these two landscape elements have been previously observed across pairs sites of the same study area [*Riveros-Iregui et al.*, 2008]; however, our results demonstrated that this magnitude difference in efflux can be consistent across multiple (62) riparian meadow locations (11) and upland sites (51) (Figure 6b). The magnitude difference between riparian meadows and upland forests is likely due to the large drainage area of riparian meadows, which results in higher and more sustained soil water content (Figure 4) and the feedback to vegetation cover (trees versus grasses) and soil characteristics. Thus, while riparian meadows in the Stringer Creek watershed comprise only 1.8% of the landscape, soil CO_2 efflux from these meadows is the highest across the entire watershed (Figure 6) and results in a disproportionate 3.5% of total catchment efflux.

[32] Cumulative soil CO_2 efflux was positively correlated with UAA (Figure 7) in upland forests, which comprised ~98% of the watershed area. This is a valuable observation, yet is to be expected given that plant and microbial activities are dependent on water availability. UAA characterizes the relative magnitude of water flow across the landscape, (i.e., drainage pattern), as highlighted in multiple studies [*Beven and Wood*, 1983; *McGlynn and Seibert*, 2003; *McGlynn et al.*, 2004; *McGuire et al.*, 2005; *Sorensen et al.*, 2006; *Seibert and McGlynn*, 2007; *Jencso et al.*, 2009], and its relationship to soil CO_2 efflux in drier areas of the landscape is an element that can be of great advantage to large-scale (~km^2) quantifications of land-atmosphere CO_2 exchange.

4.3. Scaling From Point Observations to Watershed-Scale Fluxes

[33] Currently, poor process-based understanding, sparse field measurements across space and time, and a lack of organizing principles, limit our ability to assess soil CO_2 fluxes from areas where biophysical controls (i.e., soil water content, soil temperature, vegetation cover) concurrently vary in space and time. It is well known that soil temperature can explain soil CO_2 efflux at single plots over short (diel) temporal scales [*Riveros-Iregui et al.*, 2007; *Carbone et al.*, 2008]. However, it is also well known that soil temperature and temperature-based models (e.g., Q_{10}) [*Lloyd and Taylor*, 1994] are poor predictors of soil CO_2 efflux at larger spatial scales [*Richardson and Hollinger*, 2005]. In fact, the use of temperature-based models continues to be discouraged for large scales [*Janssens and Pilegaard*, 2003; *Davidson et al.*, 2006; *Richardson et al.*, 2006], likely because soil temperature effects on soil CO_2 have been found to vary widely across ranges of soil water content conditions and drydown [*Riveros-Iregui et al.*, 2007]. Thus, it is only to be expected that systems with wide spatial differences in soil water content regimes (e.g., entire forests) and/or strong temporal differences in soil water content caused by environmental controls (e.g., snowmelt, droughts, summer drydown) will exhibit poor fits of such models. Furthermore, multiparameter models require free parameters to constrain respiration models [*Falge et al.*, 2001; *Reichstein et al.*, 2005; *Richardson and Hollinger*, 2005], which make it difficult to interpret actual physical processes. Thus, no appropriate parameter

has emerged to aid in parameterization and modeling of soil CO_2 efflux variability from large areas.

[34] Our empirical approach offers great potential across large spatial scales, comparable and useful to many other land-atmosphere studies of CO_2 exchange, and it allows for context and interpretation for plot and point scales. Our results highlight topographic organization of biogeochemical processes leading to soil CO_2 production and efflux, primarily controlled by the lateral redistribution of soil water. Using the explanatory power of UAA (~61–65%; Figure 7) as the overarching control of seasonal soil CO_2 efflux can be comparable to more complicated, multiparameter models previously developed (r^2 = 0.723) [*Webster et al.*, 2008b]. Yet the strength of the correlation of UAA and seasonal soil CO_2 efflux in combination with DEM terrain analysis tools [*Seibert and McGlynn*, 2007] and spatial integration makes our approach a crucial tool in landscape characterization and discretization and provides an important link between point-scale measurements and ecosystem/watershed-scale estimates of soil CO_2 efflux.

[35] An interesting feature that emerged in the UAA–soil CO_2 efflux relationships was the difference in the slope of regressions for sites of contrasting aspects (Figures 7b and 7c). Especially at UAA values above 1000 m^2, cumulative soil CO_2 efflux is higher in SE facing than in NW facing slopes. This difference in efflux magnitude is likely the result of higher temperatures and radiation in SE aspects leading to higher rates of root and microbial respiration. Yet this difference is not apparent among sites with UAA values below 1000 m^2, perhaps because such sites are primarily moisture limited. It is therefore to be expected that as UAA increases outside the range of moisture limitation other limitations such as aeration limitation (i.e., too much moisture like in riparian areas) will become the controlling variable on the magnitude of soil CO_2 efflux [see, e.g., *Luo and Zhou*, 2006; *Pacific et al.*, 2008]. In fact, UAA was not a good predictor of cumulative soil CO_2 efflux in riparian areas (2% of watershed area) likely because vegetation and microbial activities in these areas are less moisture limited during most of the growing season, confirming that there is a fundamental difference in processes leading to soil CO_2 production and flux between riparian areas and forested uplands as corroborated by cluster analysis of soil CO_2 effluxes as well as terrain and landscape analysis. Taken together, however, our findings reinforce the concept of concomitant effects of multiple variables occurring in space and time.

[36] Accounting for landscape heterogeneity, drainage patterns, and watershed area, our upscaled estimates of watershed-scale soil CO_2 efflux (799.45 ± 151.1 g CO_2 m^2 over 83 days) compared within ~2% of independent eddy covariance estimates of nighttime ecosystem respiration over the forest for the same period (Table 2 and Figure 9). While counteracting errors and no daytime correction in eddy covariance measurements [*Riveros-Iregui et al.*, 2008] may contribute to good agreement between these estimates, leaf-level measurements of autotrophic respiration made throughout the season demonstrated that nighttime aboveground respiration is considerably low in this ecosystem (<8%; D. Muth, unpublished data, 2006). This rationale suggests that soil CO_2 efflux represents a large component of the ecosystem respiration. While it is likely modest, the role of other types of aboveground biomass (e.g., twigs, branches, trunks) in contributing to ecosystem respiration, as well as daytime extrapolation for nighttime ecosystem respiration measurements, remain to be addressed.

[37] Nonetheless, the level of comparison between upscaled soil-based measurements that captured and accounted for structured heterogeneity, and independent tower measurements performed over the canopy forest is highly encouraging. Our study demonstrates topographic/topologic controls on the magnitude of soil CO_2 efflux in heterogeneous regions. The temporal scales of this organization remain to be tested and examined. For example, is there legacy of these topographic controls? Further investigations are warranted to address whether these dynamics are a reflection of geomorphic evolution and soil/biogeochemical development or they are simply reflections of contemporary water content and vegetation distribution.

[38] The effect of interannual climate variability on the spatial variability of soil CO_2 efflux remains unknown, and how climate variability (e.g., dry versus wet year, late snowmelt, reduced snowpack) will affect different landscape elements within a watershed or if particular elements (e.g., wet riparian meadows) are especially prone to climate variability. Our findings have important implications for quantitative assessments of soil CO_2 efflux from heterogeneous landscapes and provide a conceptual framework for soil CO_2 efflux variability based on simple landscape discretization, topographic analysis of landscape structure, and empirical relationships developed from repeated observations of soil CO_2 efflux.

4.4. Can the Shape of the Landscape (Structure) Affect the Generation and Flux of Soil CO_2 in Subalpine Ecosystems?

[39] To further our understanding of the effects of landscape structure and controls on watershed-scale soil CO_2 efflux, we created three synthetic watersheds varying in shape and slope, which were intended to represent progressively simpler models of the Stringer Creek watershed (Figure 8). Natural watersheds contain elements from these three synthetic DEMs, yet these DEMs are simplified versions of natural systems. The three synthetic watersheds are characterized as follows: (1) a symmetrical, convergent (bowl shaped) watershed; (2) a planar and steep watershed with constant slope; and (3) a planar watershed with gentler slope (Figure 8). Catchment area was comparable to the Stringer Creek watershed, and results are area normalized. For each DEM, we calculated UAA in a similar manner as for Stringer Creek DEMs described previously (section 2). We applied the same empirical model and used the same two-step approach as for Stringer Creek watershed to estimate watershed-scale soil CO_2 efflux from each synthetic DEM (Figure 9).

[40] Watershed-scale soil CO_2 efflux estimated from these synthetic watersheds was 50, 58, and 98% higher than that measured and upscaled from the Stringer Creek watershed (Figure 9b). The estimated efflux increased as watershed complexity decreased. Decreasing complexity resulted in reduced water rerouting, modifying lateral redistribution of soil water throughout each watershed. In successively simpler watersheds, UAA values progressively increased in uplands (i.e., uplands became progressively "wetter"),

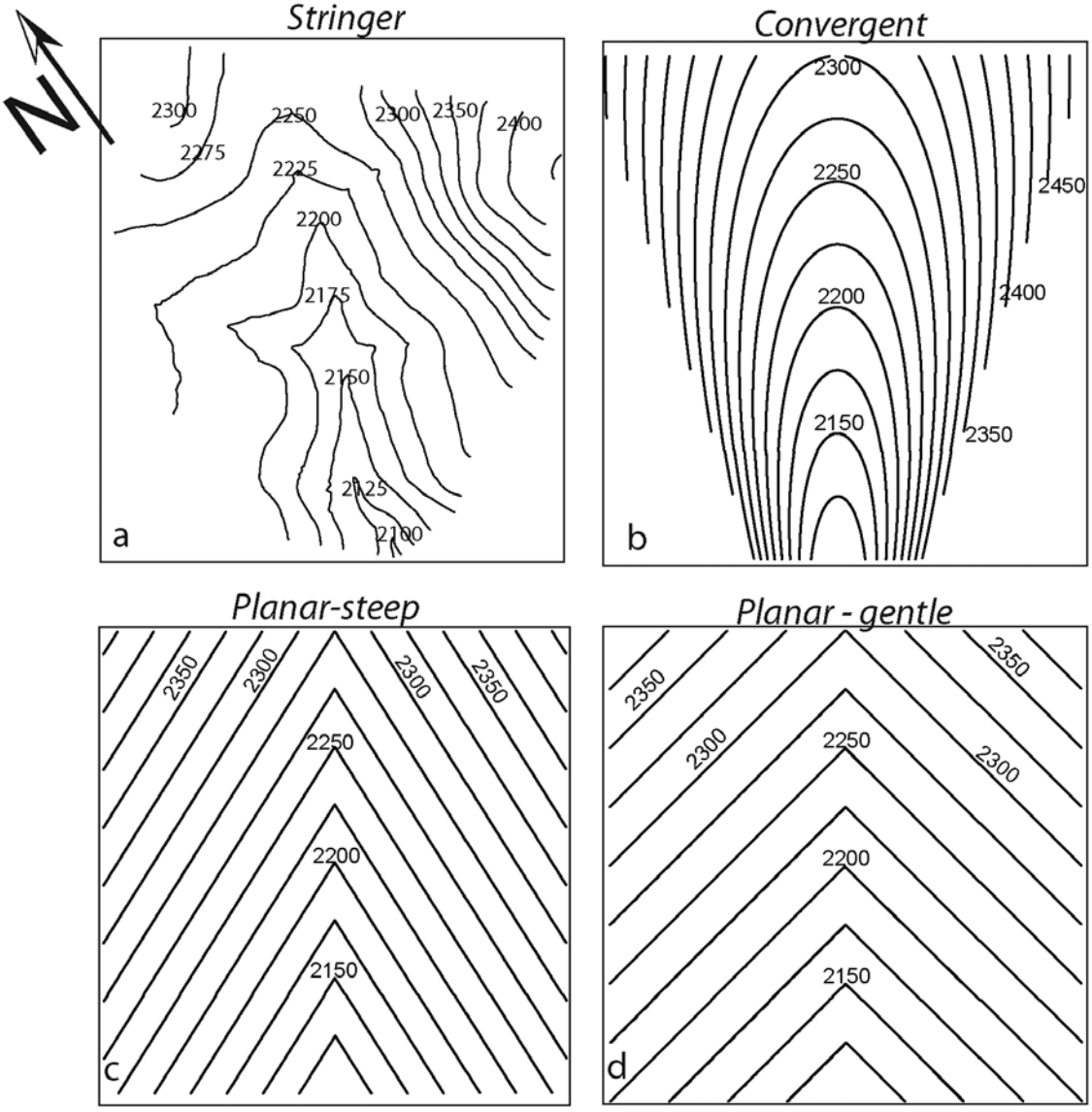

Figure 8. (a) The 25-m contours for Stringer Creek and for three synthetic digital elevation models characterized as follows: (b) a convergent watershed; (c) a planar steep watershed; and (d) a planar, gentle slope watershed. Watersheds vary in shape and slope, decreasing in terrain complexity from Figure 8a to Figure 8d.

increasing the frequency of high UAA values (Figure 9a). Natural systems exhibit heterogeneities in shape (e.g., convergence, steepness, divergence) that influence soil water redistribution, concentrating UAA (or watershed area) to lower parts of the watershed. These heterogeneities were limited in the synthetic DEMs (Figures 8b–8d), therefore the distribution of soil water was more uniform across the landscape. The least complex watershed (gentle slope; Figure 8d) exhibited the highest estimated soil CO_2 efflux, because the structure of this watershed allowed for a more homogenous distribution of UAA than the natural and other two synthetic, but more complex, watersheds.

[41] We calculated the kurtosis of the distribution of UAA values of each watershed as a metric of structural complexity. This metric allowed for intercomparison of the natural and the three synthetic watersheds (Figure 10). Although a simple metric, this analysis (Figure 10) demonstrated that for these ecosystems, landscape structure (and resulting UAA distribution) plays a major role in controlling watershed-scale rates of soil CO_2 efflux. This compelling relationship and the inherent conceptual framework warrant further investigation. Specifically, how applicable is this concept across other heterogeneous sites? What are the effects of climate variability (e.g., enhanced precipitation) on these emergent patterns in subalpine ecosystems? What are the process time scales and additional covarying variables affecting these relationships? What are the specifics of point-scale biological and physical processes across these landscape positions and how do they vary? The demonstrated correlation between landscape position/watershed structure and seasonal estimates of soil CO_2 efflux based on repeated measurements offers promise for upscaling

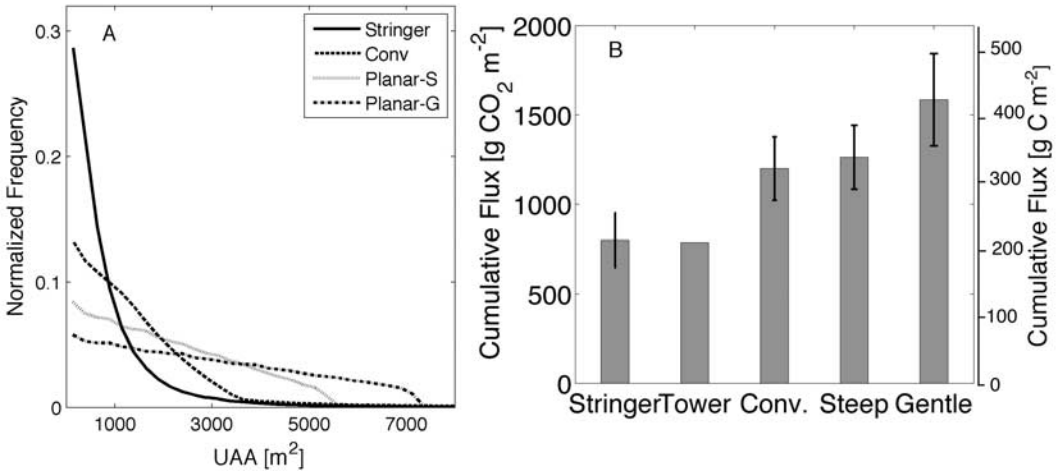

Figure 9. (a) Distribution of calculated 3-m UAA for Stringer Creek watershed and the three synthetic watersheds presented in Figure 8. (b) Seasonal soil CO_2 efflux for the same watersheds, based on the relationships found in Figure 7.

rates of soil CO_2 efflux rates from large areas, downscaling from coarser spatial measurements, and interpreting point- and plot-scale measurements and what aspects of the system they represent. Our study demonstrates that while biophysical heterogeneity is inherent in natural systems, this heterogeneity often exhibits a high degree of organization that can be of advantage to watershed and landscape scale studies.

5. Conclusions and Implications

[42] 1. Riparian meadows were found to have the highest rates of cumulative soil CO_2 efflux across the entire watershed on the basis of soil chamber measurements across 62 sites of a subalpine watershed and during the 2006 growing season. This assessment, made through two-way cluster analysis of all sites, confirmed independent riparian upland assessment made through terrain analysis and landscape delineation.

[43] 2. Empirically upscaled soil CO_2 efflux for the entire Stringer Creek watershed (799.5 ± 151.1 g CO_2 m^{-2} over 83 days) compared within 2% of independent estimates of nighttime ecosystem respiration measured over the forest canopy with the eddy covariance technique for the same period. The upscaled estimates were based on landscape discretization, topographic analysis of landscape structure, and empirical relationships developed from repeated measurements of soil CO_2 efflux.

[44] 3. Topography and landscape structure are strong indicators of the variability and magnitude of soil CO_2 efflux from complex watersheds. Landscape context and controls on heterogeneity are critical to estimation and interpretation of watershed-scale rates of soil CO_2 efflux. Landscape analysis is a critical tool for upscaling plot or point measurements to larger spatial scales, with regards to soil CO_2 efflux and likely many other biogeochemical processes mediated by soil temperature, soil water content, and the surface energy balance.

[45] 4. Modeled soil CO_2 efflux from three synthetic DEMs, varying in shape and slope with progressively less topographic complexity resulted in 50, 58, and 98% higher efflux estimates than that measured and upscaled from the Stringer Creek watershed. Decreasing complexity resulted in a more homogeneous distribution of UAA across the landscape owing to reduced flow path convergence and divergence, resulting in less lateral redistribution of soil water throughout each watershed.

[46] 5. Our results have important implications for interpreting and evaluating rates of soil CO_2 efflux from heterogeneous landscapes, and improved process understanding of watershed-scale (km^2) soil CO_2 efflux variability. This information is necessary to reduce uncertainty in ecosystem exchange of C, promote integration with other measures of ecosystem C exchange (e.g., eddy covariance in heterogeneous landscapes), and enhance parameterization and pre-

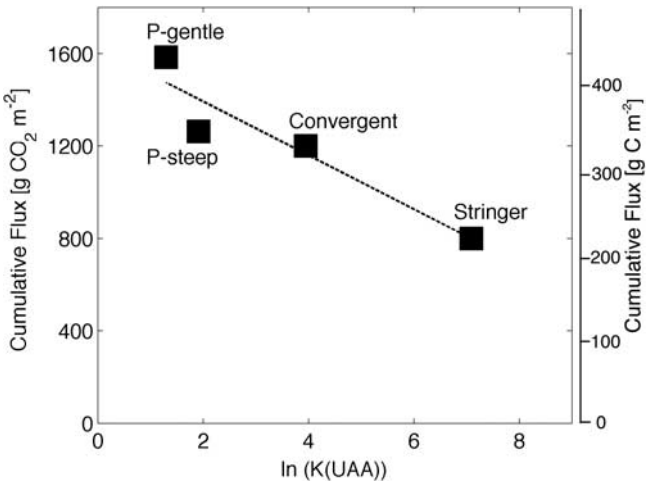

Figure 10. Relationship between the kurtosis (K) of UAA and predicted seasonal CO_2 efflux for the Stringer Creek watershed and the three synthetic cases: a convergent watershed, a planar steep watershed, and a planar gentle slope watershed.

diction of watershed-scale fluxes. These implications, and the concept of "organized heterogeneity," should be considered when measuring and modeling the dynamics of C cycling at progressively larger scales or when attempting to downscale large-scale measures.

[47] **Acknowledgments.** Financial support was provided by the U.S. National Science Foundation Integrated Carbon Cycle Research Program (grant EAR-0404130). D.A.R-I. acknowledges support from the 2007 American Geophysical Union Horton Research Grant, a NSF Doctoral Dissertation Improvement Grant (DEB-0807272), and the USGS 104b Grant Program, administered by the Montana Water Center. Airborne laser mapping was provided by the NSF supported National Center for Airborne Laser Mapping (NCALM) at the University of California, Berkeley. The authors thank the Tenderfoot Creek Experimental Forest and the USDA, Forest Service, Rocky Mountain Research Station, particularly Ward McCaughey. Field and laboratory assistance from Vince Pacific, Rebecca McNamara, Kelley Conde, Kelsey Jencso, Andres Munoz, and Austin A.P. Allen, and discussions from Howard Epstein, Daniel Welsch, Ryan Emanuel, and Dan Muth are greatly appreciated. Two anonymous reviewers and the associate editor provided valuable suggestions for the improvement of this manuscript.

References

Baldocchi, D. D. (2003), Assessing the eddy covariance technique for evaluating carbon dioxide exchange rates of ecosystems: Past, present and future, *Global Change Biol.*, *9*(4), 479–492, doi:10.1046/j.1365-2486.2003.00629.x.

Beven, K. J., and M. J. Kirkby (1979), A physically based, variable contributing area model of basin hydrology, *Hydrol. Sci. Bull.*, *24*(1), 43–69.

Beven, K., and E. F. Wood (1983), Catchment geomorphology and the dynamics of runoff contributing areas, *J. Hydrol.*, *65*(1–3), 139–158, doi:10.1016/0022-1694(83)90214-7.

Beven, K. J., K. Gilman, and M. Newson (1979), Flow and flow routing in upland channel networks, *Hydrol. Sci. Bull.*, *24*(3), 303–325.

Bosatta, E., and H. Staaf (1982), The control of nitrogen turn-over in forest litter, *Oikos*, *39*(2), 143–151, doi:10.2307/3544478.

Burt, T. P., and D. P. Butcher (1985), Topographic controls of soil moisture distributions, *J. Soil Sci.*, *36*(3), 469–486, doi:10.1111/j.1365-2389.1985.tb00351.x.

Burton, A. J., K. S. Pregitzer, and R. L. Hendrick (2000), Relationships between fine root dynamics and nitrogen availability in Michigan northern hardwood forests, *Oecologia*, *125*(3), 389–399, doi:10.1007/s004420000455.

Carbone, M. S., G. C. Winston, and S. E. Trumbore (2008), Soil respiration in perennial grass and shrub ecosystems: Linking environmental controls with plant and microbial sources on seasonal and diel timescales, *J. Geophys. Res.*, *113*, G02022, doi:10.1029/2007JG000611.

Davidson, E. A., I. A. Janssens, and Y. Q. Luo (2006), On the variability of respiration in terrestrial ecosystems: Moving beyond Q(10), *Global Change Biol.*, *12*(2), 154–164, doi:10.1111/j.1365-2486.2005.01065.x.

Enriquez, S., C. M. Duarte, and K. Sandjensen (1993), Patterns in decomposition rates among photosynthetic organisms: The importance of detritus C-N-P content, *Oecologia*, *94*(4), 457–471, doi:10.1007/BF00566960.

Falge, E., et al. (2001), Gap filling strategies for defensible annual sums of net ecosystem exchange, *Agric. For. Meteorol.*, *107*(1), 43–69, doi:10.1016/S0168-1923(00)00225-2.

Famiglietti, J. S., and E. F. Wood (1991), Evapotranspiration and runoff from large land areas: Land surface hydrology for atmospheric general-circulation models, *Surv. Geophys.*, *12*(1–3), 179–204, doi:10.1007/BF01903418.

Farnes, P. E., R. C. Shearer, W. W. McCaughey, and K. J. Hansen (1995), Comparisons of hydrology, geology, and physical characteristics between Tenderfoot Creek Experimental Forest (east side) Montana, and Coram Experimental Forest (west side) Montana, *Final Rep. RJVA-INT-92734*, 19 pp., USDA For. Serv., Intermountain Res. Stn., For. Sci. Lab., Bozeman, Mont.

Fierer, N., B. P. Colman, J. P. Schimel, and R. B. Jackson (2006), Predicting the temperature dependence of microbial respiration in soil: A continental-scale analysis, *Global Biogeochem. Cycles*, *20*, GB3026, doi:10.1029/2005GB002644.

Fox, A. M., B. Huntley, C. R. Lloyd, M. Williams, and R. Baxter (2008), Net ecosystem exchange over heterogeneous Arctic tundra: Scaling between chamber measurements and eddy covariance measurements, *Global Biogeochem. Cycles*, *22*, GB2027, doi:10.1029/2007GB003027.

Goulden, M. L., J. W. Munger, S. M. Fan, B. C. Daube, and S. C. Wofsy (1996), Measurements of carbon sequestration by long-term eddy covariance: Methods and a critical evaluation of accuracy, *Global Change Biol.*, *2*(3), 169–182, doi:10.1111/j.1365-2486.1996.tb00070.x.

Grayson, R., and A. Western (2001), Terrain and the distribution of soil moisture, *Hydrol. Processes*, *15*(13), 2689–2690, doi:10.1002/hyp.479.

Guntner, A., J. Seibert, and S. Uhlenbrook (2004), Modeling spatial patterns of saturated areas: An evaluation of different terrain indices, *Water Resour. Res.*, *40*, W05114, doi:10.1029/2003WR002864.

Heikkinen, J. E. P., T. Virtanen, J. T. Huttunen, V. Elsakov, and P. J. Martikainen (2004), Carbon balance in East European tundra, *Global Biogeochem. Cycles*, *18*, GB1023, doi:10.1029/2003GB002054.

Hollinger, D. Y., F. M. Kelliher, J. N. Byers, J. E. Hunt, T. M. McSeveny, and P. L. Weir (1994), Carbon dioxide exchange between an undisturbed old-growth temperate forest and the atmosphere, *Ecology*, *75*(1), 134–150, doi:10.2307/1939390.

Jacobs, C. M. J., et al. (2007), Variability of annual CO_2 exchange from Dutch grasslands, *Biogeosciences*, *4*(5), 803–816.

Janssens, I. A., and K. Pilegaard (2003), Large seasonal changes in Q(10) of soil respiration in a beech forest, *Global Change Biol.*, *9*(6), 911–918, doi:10.1046/j.1365-2486.2003.00636.x.

Jencso, K. G., B. L. McGlynn, M. N. Gooseff, S. M. Wondzell, and K. E. Bencala (2009), Hydrologic connectivity between landscapes and streams: Transferring reach and plot scale understanding to the catchment scale, *Water Resour. Res.*, *45*, W04428, doi:10.1029/2008WR007225.

Kang, S. Y., S. Doh, D. Lee, V. L. Jin, and J. S. Kimball (2003), Topographic and climatic controls on soil respiration in six temperate mixed-hardwood forest slopes, Korea, *Global Change Biol.*, *9*(10), 1427–1437, doi:10.1046/j.1365-2486.2003.00668.x.

Kang, S., D. Lee, J. Lee, and S. W. Running (2006), Topographic and climatic controls on soil environments and net primary production in a rugged temperate hardwood forest in Korea, *Ecol. Res.*, *21*(1), 64–74, doi:10.1007/s11284-005-0095-0.

Kim, J., Q. Guo, D. D. Baldocchi, M. Leclerc, L. Xu, and H. P. Schmid (2006), Upscaling fluxes from tower to landscape: Overlaying flux footprints on high-resolution (IKONOS) images of vegetation cover, *Agric. For. Meteorol.*, *136*(3–4), 132–146, doi:10.1016/j.agrformet.2004.11.015.

Korkalainen, T., and A. Lauren (2006), Using phytogeomorphology, cartography forest site productivity expressed and GIS to explain as tree height in southern and central Finland, *Geomorphology*, *74*(1–4), 271–284, doi:10.1016/j.geomorph.2005.09.001.

Larsen, K. S., A. Ibrom, C. Beier, S. Jonasson, and A. Michelsen (2007), Ecosystem respiration depends strongly on photosynthesis in a temperate heath, *Biogeochemistry*, *85*(2), 201–213, doi:10.1007/s10533-007-9129-8.

Lavigne, M. B., et al. (1997), Comparing nocturnal eddy covariance measurements to estimates of ecosystem respiration made by scaling chamber measurements at six coniferous boreal sites, *J. Geophys. Res.*, *102*, 28,977–28,985, doi:10.1029/97JD01173.

Lloyd, J., and J. A. Taylor (1994), On the temperature-dependence of soil respiration, *Funct. Ecol.*, *8*(3), 315–323, doi:10.2307/2389824.

Lookingbill, T., and D. Urban (2004), An empirical approach towards improved spatial estimates of soil moisture for vegetation analysis, *Landscape Ecol.*, *19*(4), 417–433, doi:10.1023/B:LAND.0000030451.29571.8b.

Luo, Y., and X. Zhou (2006), *Soil Respiration and the Environment*, Elsevier, New York.

Maier, C. A., and L. W. Kress (2000), Soil CO_2 evolution and root respiration in 11 year-old loblolly pine (Pinus taeda) plantations as affected by moisture and nutrient availability, *Can. J. For. Res.*, *30*(3), 347–359, doi:10.1139/cjfr-30-3-347.

McGlynn, B. L., and J. Seibert (2003), Distributed assessment of contributing area and riparian buffering along stream networks, *Water Resour. Res.*, *39*(4), 1082, doi:10.1029/2002WR001521.

McGlynn, B. L., J. J. McDonnell, J. Seibert, and C. Kendall (2004), Scale effects on headwater catchment runoff timing, flow sources, and groundwater-streamflow relations, *Water Resour. Res.*, *40*, W07504, doi:10.1029/2003WR002494.

McGuire, K. J., J. J. McDonnell, M. Weiler, C. Kendall, B. L. McGlynn, J. M. Welker, and J. Seibert (2005), The role of topography on catchment-scale water residence time, *Water Resour. Res.*, *41*, W05002, doi:10.1029/2004WR003657.

Mincemoyer, S. A., and J. L. Birdsall (2006), Vascular flora of the Tenderfoot Creek Experimental Forest, Little Belt Mountains, Montana, *Madrono*, *53*(3), 211–222, doi:10.3120/0024-9637(2006)53[211:VFOTTC]2.0.CO;2.

Norman, J. M., R. Garcia, and S. B. Verma (1992), Soil surface CO_2 fluxes and the carbon budget of a grassland, *J. Geophys. Res.*, *97*, 18,845–18,853.

Nouvellon, Y., et al. (2008), Soil CO_2 effluxes, soil carbon balance, and early tree growth following savannah afforestation in Congo: Comparison

of two site preparation treatments, *For. Ecol. Manage.*, *255*(5–6), 1926–1936, doi:10.1016/j.foreco.2007.12.026.

Pacific, V. J., B. L. McGlynn, D. A. Riveros-Iregui, D. L. Welsch, and H. E. Epstein (2008), Variability in soil respiration across riparian-hillslope transitions, *Biogeochemistry*, *91*, 51–70, doi:10.1007/s10533-008-9258-8.

Pierce, K. B., T. Lookingbill, and D. Urban (2005), A simple method for estimating potential relative radiation (PRR) for landscape-scale vegetation analysis, *Landscape Ecol.*, *20*(2), 137–147, doi:10.1007/s10980-004-1296-6.

Pregitzer, K. S., J. A. King, A. J. Burton, and S. E. Brown (2000), Responses of tree fine roots to temperature, *New Phytol.*, *147*(1), 105–115, doi:10.1046/j.1469-8137.2000.00689.x.

Raich, J. W., and C. S. Potter (1995), Global patterns of carbon-dioxide emissions from soils, *Global Biogeochem. Cycles*, *9*(1), 23–36, doi:10.1029/94GB02723.

Raich, J. W., and W. H. Schlesinger (1992), The global carbon-dioxide flux in soil respiration and its relationship to vegetation and climate, *Tellus, Ser. B*, *44*(2), 81–99, doi:10.1034/j.1600-0889.1992.t01-1-00001.x.

Randerson, J. T., et al. (2002), Carbon isotope discrimination of arctic and boreal biomes inferred from remote atmospheric measurements and a biosphere-atmosphere model, *Global Biogeochem. Cycles*, *16*(3), 1028, doi:10.1029/2001GB001435.

Reichstein, M., et al. (2005), On the separation of net ecosystem exchange into assimilation and ecosystem respiration: Review and improved algorithm, *Global Change Biol.*, *11*(9), 1424–1439, doi:10.1111/j.1365-2486.2005.001002.x.

Richardson, A. D., and D. Y. Hollinger (2005), Statistical modeling of ecosystem respiration using eddy covariance data: Maximum likelihood parameter estimation, and Monte Carlo simulation of model and parameter uncertainty, applied to three simple models, *Agric. For. Meteorol.*, *131*(3–4), 191–208, doi:10.1016/j.agrformet.2005.05.008.

Richardson, A. D., et al. (2006), Comparing simple respiration models for eddy flux and dynamic chamber data, *Agric. For. Meteorol.*, *141*(2–4), 219–234, doi:10.1016/j.agrformet.2006.10.010.

Riveros-Iregui, D. A. (2008), Hydrologic-carbon cycle linkages in a subalpine catchment, Ph.D. dissertation, 220 pp., Montana State Univ., Bozeman.

Riveros-Iregui, D. A., R. E. Emanuel, D. J. Muth, B. L. McGlynn, H. E. Epstein, D. L. Welsch, V. J. Pacific, and J. M. Wraith (2007), Diurnal hysteresis between soil CO_2 and soil temperature is controlled by soil water content, *Geophys. Res. Lett.*, *34*, L17404, doi:10.1029/2007GL030938.

Riveros-Iregui, D. A., B. L. McGlynn, H. E. Epstein, and D. L. Welsch (2008), Interpretation and evaluation of combined measurement techniques for soil CO_2 efflux: Surface chambers and soil CO_2 concentration probes, *J. Geophys. Res.*, *113*, G04027, doi:10.1029/2008JG000811.

Rodhe, A., and J. Seibert (1999), Wetland occurrence in relation to topography: A test of topographic indices as moisture indicators, *Agric. For. Meteorol.*, *98–99*, 325–340, doi:10.1016/S0168-1923(99)00104-5.

Ryan, M. G., M. B. Lavigne, and S. T. Gower (1997), Annual carbon cost of autotrophic respiration in boreal forest ecosystems in relation to species and climate, *J. Geophys. Res.*, *102*, 28,871–28,883, doi:10.1029/97JD01236.

Saiz, G., C. Green, K. Butterbach-Bahl, R. Kiese, V. Avitabile, and E. P. Farrell (2006), Seasonal and spatial variability of soil respiration in four sitka spruce stands, *Plant Soil*, *287*(1–2), 161–176, doi:10.1007/s11104-006-9052-0.

Schimel, D. S., T. G. F. Kittel, S. W. Running, R. K. Monson, A. Turnipseed, and D. Anderson (2002), Carbon sequestration studied in wertern U.S. mountains, *Eos Trans. AGU*, *83*(40), 445–449, doi:10.1029/2002EO000314.

Scott-Denton, L. E., K. L. Sparks, and R. K. Monson (2003), Spatial and temporal controls of soil respiration rate in a high-elevation, subalpine forest, *Soil Biol. Biochem.*, *35*(4), 525–534, doi:10.1016/S0038-0717(03)00007-5.

Scott-Denton, L. E., T. N. Rosenstiel, and R. K. Monson (2006), Differential controls by climate and substrate over the heterotrophic and rhizospheric components of soil respiration, *Global Change Biol.*, *12*(2), 205–216, doi:10.1111/j.1365-2486.2005.01064.x.

Seibert, J., and B. L. McGlynn (2007), A new triangular multiple flow direction algorithm for computing upslope areas from gridded digital elevation models, *Water Resour. Res.*, *43*, W04501, doi:10.1029/2006WR005128.

Shibistova, O., et al. (2002), Seasonal and spatial variability in soil CO_2 efflux rates for a central Siberian Pinus sylvestris forest, *Tellus, Ser. B*, *54*(5), 552–567, doi:10.1034/j.1600-0889.2002.01348.x.

Soegaard, H., C. Nordstroem, T. Friborg, B. U. Hansen, T. R. Christensen, and C. Bay (2000), Trace gas exchange in a high-arctic valley: 3. Integrating and scaling CO_2 fluxes from canopy to landscape using flux data, footprint modeling, and remote sensing, *Global Biogeochem. Cycles*, *14*(3), 725–744, doi:10.1029/1999GB001137.

Sorensen, R., U. Zinko, and J. Seibert (2006), On the calculation of the topographic wetness index: Evaluation of different methods based on field observations, *Hydrol. Earth Syst. Sci.*, *10*(1), 101–112.

Spath, H. (1985), *Cluster Dissection and Analysis: Theory, FORTRAN Programs, Examples*, 226 pp., Ellis Horwood, New York.

Stage, A. R. (1976), Expression for effect of aspect, slope, and habitat type on tree growth, *For. Sci. [Washington D. C.]*, *22*(4), 457–460.

Tang, J. W., L. Misson, A. Gershenson, W. X. Cheng, and A. H. Goldstein (2005), Continuous measurements of soil respiration with and without roots in a ponderosa pine plantation in the Sierra Nevada Mountains, *Agric. For. Meteorol.*, *132*(3–4), 212–227, doi:10.1016/j.agrformet.2005.07.011.

Urban, D. L., C. Miller, P. N. Halpin, and N. L. Stephenson (2000), Forest gradient response in Sierran landscapes: The physical template, *Landscape Ecol.*, *15*(7), 603–620, doi:10.1023/A:1008183331604.

Valentini, R., et al. (2000), Respiration as the main determinant of carbon balance in European forests, *Nature*, *404*(6780), 861–865, doi:10.1038/35009084.

Vargas, R., and M. F. Allen (2008), Diel patterns of soil respiration in a tropical forest after Hurricane Wilma, *J. Geophys. Res.*, *113*, G03021, doi:10.1029/2007JG000620.

Vourlitis, G. L., W. C. Oechel, A. Hope, D. Stow, B. Boynton, J. Verfaillie, R. Zulueta, and S. J. Hastings (2000), Physiological models for scaling plot measurements of CO_2 flux across an arctic tundra landscape, *Ecol. Appl.*, *10*(1), 60–72.

Webster, K. L., I. F. Creed, F. D. Beall, and R. A. Bourbonniere (2008a), Sensitivity of catchment-aggregated estimates of soil carbon dioxide efflux to topography under different climate conditions, *J. Geophys. Res.*, *113*, G03040, doi:10.1029/2008JG000707.

Webster, K. L., I. F. Creed, R. A. Bourbonniere, and F. D. Beall (2008b), Controls on the heterogeneit of soil respiration in a tolerant hardwood forest, *J. Geophys. Res.*, *113*, G03018, doi:10.1029/2008JG000706.

Western, A. W., and R. B. Grayson (1998), The Tarrawarra data set: Soil moisture patterns, soil characteristics, and hydrological flux measurements, *Water Resour. Res.*, *34*, 2765–2768, doi:10.1029/98WR01833.

Western, A. W., G. Bloeschl, and R. B. Grayson (1998), Geostatistical characterisation of soil moisture patterns in the Tarrawarra catchment, *J. Hydrol.*, *205*(1–2), 20–37, doi:10.1016/S0022-1694(97)00142-X.

Western, A. W., R. B. Grayson, G. Blöschl, G. R. Willgoose, and T. A. McMahon (1999), Observed spatial organization of soil moisture and its relation to terrain indices, *Water Resour. Res.*, *35*, 797–810, doi:10.1029/1998WR900065.

Woods, S. W., R. Ahl, J. Sappington, and W. McCaughey (2006), Snow accumulation in thinned lodgepole pine stands, Montana, USA, *For. Ecol. Manage.*, *235*(1–3), 202–211, doi:10.1016/j.foreco.2006.08.013.

Zinko, U., J. Seibert, M. Dynesius, and C. Nilsson (2005), Plant species numbers predicted by a topography-based groundwater flow index, *Ecosystems*, *8*(4), 430–441.

B. L. McGlynn, Department of Land Resources and Environmental Sciences, Montana State University, 334 Leon Johnson Hall, Bozeman, MT 59717, USA.

D. A. Riveros-Iregui, Department of Ecology and Evolutionary Biology, University of Colorado, 334 UCB, Boulder, CO 80309, USA. (riveros@Colorado.edu)